

Double Star Measurements with Robotic Telescope and AstroimageJ

Zsolt Szamosvari
Hungarian Astronomical Association Double Star Section
H-2500 Esztergom, Hungary;
szamos.photo@gmail.com

Abstract

In the last couple of months, I have measured 160 double stars with the help of images taken with a robotic telescope. These are mostly multiple systems, which are included in the WDS with measurement results that are 7-8 years old or older. Many of them are among the rarely observed objects. A new double star with the coordinates 18 00 53,13 +56 24 27,20 could also be found.

1. Introduction

I've been observing double stars since 2003, and in the last half year I've been using a robotic telescope to achieve greater accuracy. My observations are published by the local astronomy newspaper, and I wrote this paper on their behalf.

2. Equipment and Methods

I took 10 pictures of different areas of the sky with iTelescope.net's robotic telescopes, each with an exposure time of 90 seconds. I found that this exposure time burns out the bright stars even less, but the fainter stars are visible down to about 18 magnitude. If one of the stars burns out, reducing the contrast to a certain extent helps to display the closer companions. For the measurements, I used "calibrated" images taken by the telescope. These are automatically processed by the telescope's internal software (dark, flat, bias subtraction).

The measurements were made with the AstroimageJ software (Harfenist, 2018). I imported the images in the AstroimageJ software. After the import, the software performs astrometric calibration on each image based on astrometry.net and the metadata of the images. In this case, it not only identifies the objects visible in the image and gives their coordinates, but also defines the image skies. I still have to enter the mapping data of each camera in the software, so the measurements on the images will be accurate.

The accuracy of the software measurement decreases in the case of close pairs. The standard deviation of the separation measurement for wider pairs is less than ± 0.15 arcseconds. In the case of close ($>5''$) pairs, however, this can be up to ± 1 second of arc. The standard deviation of the position angle measurement depends on the degree of separation. In the case of close ($>5''$) pairs, this can be even $\pm 1^\circ$. For each pair, I took the average of 10 measurements, which I rounded to 2 decimal places.

Where I found a greater deviation from the WDS data, I used the Plot_Tool 3.19 Excel spreadsheet to check my measurements (Harshaw 2020).

Table 1. Used telescopes.

Telescope No	T02	T33	T68
OTA	Takahashi TOA-150	12.5" - 320mm RCOS	Celestron RASA 11" 280mm
Optical Design	Apochromatic Refractor	Ritchey-Chrétien	Rowe Ackerman Schmidt Astrograph
Aperture	150 mm	320 mm	279 mm
Focal Length	1105.1 mm	2885 mm	620 mm
F/Ratio	f7.3	f/9	f/2.2
CCD	QHY268C, CMOS	Apogee Alta U16	ZWO ASI2600 Color
Resolution	0.705 "/px	0.66 "/px	1.25 "/px
Normal Array	6280x4210 px	4090x4096 px	6248X4176
FOV	72.6'x48.6'	37'x37'	130,2'x87'
Location	New Mexico, USA	Siding Springs, Australia	New Mexico, USA

3. Data

The following table shows the measurements of separation and position angle of 160 double stars. The brightness and coordinates are taken from The Washington Double Star Catalog (Mason et al., 2020) Date is given in Julian years. Where I have not indicated it separately, the photograph was taken by the T33 telescope.

Table 2. Measurements

WDS CODE	NAME	MAGS	SEP "	PA °	DATE	NOTES
02094-1011	HJ 2116 AB	9.68/14.25	27.51	150.34	2022.220	See sec. 3.1.
02470-0952	STF 308 AB,CD	9.79/10.43	21.00	334.14	2022.198	See sec. 3.2.
16253-4038	SEE 274 AB	9.57/12.10	5.59	240.15	2022.201	
	SEE 274 AC	9.57/14.10	12.70	291.36	2022.201	
	SEE 274 AD	9.57/13.10	26.52	252.81	2022.201	
16260-4051	SEE 275	9.70/14.20	11.88	179.22	2022.201	
16479-4058	LDS 570 AB	8.25/11.57	24.36	161.90	2022.222	
	SIN 98 BC	11.57/13.60	90.38	70.30	2022.222	
	SIN 98 BD	11.57/12.72	103.09	289.54	2022.222	
16541-4151	SEE 295	8.72/9.70	5.91	14.29	2022.202	

16542-4150	SEE 297 AB	6.07/9.86	13.19	129.79	2022.202	V 1007 Sco; See sec. 3.3.
	SEE 297 AC	6.07/11.50	23.10	121.90	2022.202	
	SEE 300 DE	9.50/11.90	7.77	265.09	2022.202	
16542-4151	WFC 183 AB	6.39/7.74	30.98	35.10	2022.202	
16543-4150	B 1835	8.80/13.40	3.47	256.48	2022.202	
16544-4150	HJ 4893	7.44/9.60	7.33	51.82	2022.202	
16551-4205	SEE 303	6.35/9.70	21.81	164.28	2022.202	
17190-3459	HJ 4935 AC	6.37/10.27	32.60	141.69	2022.221	See sec. 3.4.
	SEE 509 AD	6.37/12.45	91.99	284.73	2022.221	
	SEE 509 CD	10.27/12.45	119.71	294.19	2022.221	
18029+5626	STF 2278 AB	7.78/8.14	35.06	30.87	2022.225	T68
	STF 2278 AD	7.78/10.19	197.91	188.51	2022.225	T68
	SLE 128 AE	7.78/13.18	46.41	279.01	2022.225	T68
	SLE 128 AF	7.78/12.72	85.15	277.52	2022.225	T68
	SLE 128 AG	7.78/11.96	127.19	250.01	2022.225	T68
	STF 2278 DS	10.19/14.60	6.67	212.77	2022.225	T68
18176-3406	HJ 5036 AB	6.03/9.48	38.74	85.17	2022.209	RS Sgr, See sec.3.5.
	HJ 5036 AC	6.03/8.70	93.77	40.54	2022.209	
	HJ 5036 CD	8.70/10.20	22.37	346.24	2022.209	
18239-3421	ARY 76	11.00/11.60	18.91	9.75	2022.197	
18242-3423	SEE 351 AB	1.85/14.30	39.91	313.85	2022.197	See sec. 3.6.
	TOK 617 AD	1.85/9.03	862.92	35.67	2022.197	

18248-3424	SKF 2065	8.30/11.00	23.27	164.17	2022.197	
18468+1812	DAM 351	12.40/13.50	9.19	193.11	2022.219	T02
18470+1811	ENG 64 AB	4.36/11.60	113.69	240.54	2022.219	T02; 111 Her
	ENG 64 AC	4.36/10.53	135.80	252.39	2022.219	T02
	ENG 64 AD	4.36/11.46	143.78	258.03	2022.219	T02
	ENG 64 BC	11.60/10.53	33.75	295.89	2022.219	T02
18470+1811	ABH 103 BE	11.60/12.85	85.94	287.84	2022.219	T02
	ABH 103 BF	11.60/13.41	112.51	262.56	2022.219	T02
	ABH 103 BG	11.60/13.76	63.83	134.95	2022.219	T02
	ABH 103 BH	11.60/15.27	92.90	324.99	2022.219	T02
	ABH 103 BI	11.60/14.83	139.88	245.75	2022.219	T02
	SMA 80 CD	10.53/11.46	18.41	313.13	2022.219	T02
	ENG 64 DJ	11.46/11.92	132.42	252.64	2022.219	T02
18473+1806	DAM 352	12.70/13.60	11.36	201.66	2022.219	T02
18487+1803	BPM 840	14.49/14.54	102.96	10257	2022.219	T02
18492+1813	SMA 81 AB	11.23/11.65	21.87	338.32	2022.219	T02; See sec.3.7.
	DAM 353 AD	11.23/13.00	9.63	258.80	2022.219	T02
18579-2524	B 2871 AB	9.61/11.60	14.67	296.41	2022.213	
	SIN 112 AC	9.61/13.34	54.34	94.33	2022.213	
19163+0438	HJ 880	11.90/12.10	10.27	115.91	2022.198	T02
19188+0451	BAL 2938	9.70/10.70	9.58	91.05	2022.198	T02
19288+0809	HJ 2873 AB	10.82/12.30	8.98	301.33	2022.218	T02

	HJ 2873 AC	10.82/12.70	12.96	198.71	2022.218	T02
	ABH 118 AD	10.79/15.40	10.87	17.56	2022.218	T02
	ABH 118 AE	10.79/14.74	19.95	339.09	2022.218	T02
	ABH 118 AF	10.79/14.40	78.58	327.06	2022.218	T02
	ABH 118 AG	10.79/12.64	99.92	301.37	2022.218	T02
	ABH 118 AH	10.79/12.70	88.53	280.40	2022.218	T02
19288+0809	ABH 118 AI	10.79/14.90	105.98	103.85	2022.218	T02
	ABH 118 AJ	10.79/15.40	69.14	123.70	2022.218	T02
19294+2748	OL 217	10.56/11.05	7.54	253.62	2022.219	T02
19304+2806	KPP 895	12.40/12.90	7.46	103.84	2022.219	T02
19307+2758	SMR 34 AH	3.19/12.50	54.48	116.78	2022.219	T02
	SMR 34 AI	3.19/12.50	37.52	131.33	2022.219	T02
	SMR 34 AJ	3.19/10.00	146.31	132.35	2022.219	T02
	SMR 34 AK	3.19/11.50	141.86	277.23	2022.219	T02
	STFA 43 AB	3.19/4.68	34.64	53.65	2022.219	T02; Albireo; See sec.3.8.
	WAL 114 AC	3.19/10.99	65.23	340.79	2022.219	T02
	CTT 17 AD	3.19/12.24	108.23	32.34	2022.219	T02
	CTT 17 AE	3.19/11.81	75.34	205.56	2022.219	T02
	SMR 34 AF	3.19/12.00	59.14	45.36	2022.219	T02
	SMR 34 AG	3.19/12.50	162.80	44.52	2022.219	T02
19315+2808	ES 485	10.41/11.70	3.01	332.37	2022.219	T02
19321+2816	BU 652 AB	7.67/13.30	5.03	312.93	2022.219	T02

	STF 2539 AC	7.67/9.78	5.27	4.09	2022.219	T02; See sec. 3.9.
	FOX 242 AD	7.67/12.02	55.29	242.33	2022.219	T02
	STF 2539 BC	13.30/9.78	5.52	65.13	2022.219	T02
	FOX 242 DE	11.30/13.30	6.41	225.22	2022.219	T02
19439-1621	KPP 1943	12.40/12.90	15.38	41.18	2022.219	
20140+3726	SLE 969	13.00/13.00	9.07	254.47	2022.204	T02
20141+3755	SEI 1033	9.74/12.73	20.00	341.91	2022.204	T02
20142+3750	SEI 1034	9.70/11.77	26.09	58.91	2022.204	T02
20150+3729	KPP 2316	11.80/14.70	19.33	227.25	2022.204	T02
20158+3759	SLE 978	12.50/12/49	11.80	198.19	2022.204	T02
20160+3758	SEI 1048	11.96/11.96	19.64	121.36	2022.204	T02
20161+3738	SLE 980	9.90/12.50	14.18	225.92	2022.204	T02
20162+3745	TOB 183	11.32/13.78	14.69	256.17	2022.204	T02
20165+3739	BU 442 AB	9.72/8.04	18.31	102.75	2022.204	T02
	SLV 8 AC	9.72/8.82	31.38	77.03	2022.204	T02
	AGH 135 AD	9.72/12.60	24.39	49.25	2022.204	T02
	SLE 982 AG	9.72/10.61	24.39	49.25	2022.204	T02
	SLE 982 AH	9.72/13.47	111.64	18.60	2022.204	T02
	SLE 982 AI	9.72/13.50	63.24	43.42	2022.204	T02
	SLE 982 AJ	9.72/13.10	96.52	34.22	2022.204	T02
	SLE 982 AK	9.72/11.49	114.89	33.72	2022.204	T02
	SLE 982 AL	9.72/9.49	177.32	27.29	2022.204	T02

	SLE 982 AM	9.72/13.20	88.94	65.21	2022.204	T02
	SLE 982 AN	9.72/12.41	155.93	76.08	2022.204	T02
	SLE 982 AO	9.72/12.70	58.73	118.30	2022.204	T02
	BU 442 AP	9.72/10.80	4.74	154.58	2022.204	T02
	BU 442 AQ	9.72/13.10	8.73	155.92	2022.204	T02
	BU 442 AR	9.72/11.07	19.20	331.55	2022.204	T02
20165+3739	BU 442 BC	8.04/8.82	16.91	48.97	2022.204	T02
	BU 442 BD	8.04/12.60	20.05	1.87	2022.204	T02
	ABH 135 BE	8.04/12.89	50.22	87.96	2022.204	T02
	ABH 135 BF	8.04/12.46	64.37	139.4	2022.204	T02
	ABH 135 BO	8.04/12.70	41.48	125.03	2022.204	T02
	BU 442 BP	8.04/10.80	16.53	268.51	2022.204	T02
	BU 442 BR	8.04/11.07	34.38	307.75	2022.204	T02
	BU 442 BT	8.04/11.50	6.46	161.97	2022.204	T02
	BU 442 BU	8.04/11.50	25.69	74.14	2022.204	T02
	BU 442 BV	8.04/12.00	31.31	85.95	2022.204	T02
	BU 442 CD	8.82/12.60	15.05	306.29	2022.204	T02
	BU 442 CU	8.82/11.50	12.65	108.90	2022.204	T02
	BU 442 CV	8.82/12.00	20.43	115.75	2022.204	T02
	BU 442 UV	11.50/12.00	8.02	126.60	2022.204	T02
20166+3759	ALI 663	12.70/13.00	12.01	58.03	2022.204	T02
20168+3731	ARY 25	8.65/8.72	147.08	293.20	2022.204	T02

20168+3755	SLE 984	12.80/14.10	8.19	174.65	2022.204	T02
20169+3743	SLE 985	11.36/13.70	14.09	186.04	2022.204	T02
20171+3738	SLE 986 AB	10.78/15.10	6.36	346.52	2022.204	T02
	SLE 986 AC	10.78/12.40	17.90	1.22	2022.204	T02
20171+3740	SLE 989	12.30/13.60	8.91	222.98	2022.204	T02
20176+3729	SLE 987	10.90/11.70	11.09	207.95	2022.204	T02
20187+3720	SLE 995	11.60/11.60	8.83	143.23	2022.204	T02
20189+3723	BKO 823	11.90/12.90	6.44	201.43	2022.204	T02
20258-0154	HJ 2960	12.06/14.10	13.22	232.28	2022.218	T02
20275-0206	S 749 AB	6.76/7.51	59.96	188.55	2022.218	T02
	S 749 AC	6.76/11.30	45.59	328.62	2022.218	T02
	S 749 AD	6.76/12.37	89.88	269.36	2022.218	T02
	S 749 CD	10.80/11.00	77.53	238.66	2022.218	T02
	S 749 CE	10.80/13.70	18.78	197.17	2022.218	T02
	S 749 DF	11.00/13.60	6.69	26.34	2022.217	T02
21052+3838	ALI 958	10.58/12.70	8.07	145.81	2022.209	T02
21069+3845	STF 2758 AB	5.20/6.05	31.90	153.44	2022.204	T02; 61 Cyg
	STF 2758 AC	5.35/10.23	871.47	219.94	2022.204	T02
	STF 2758 AD	5.35/10.45	780.5	249.50	2022.204	T02
	STF 2758 AE	5.35/9.63	365.4	263.99	2022.204	T02
	STF 2758 AF	5.35/11.30	402.86	239.57	2022.204	T02
	STF 2758 AG	5.35/11.30	292.01	235.42	2022.204	T02

	STF 2758 AH	5.35/9.97	138.06	261.80	2022.204	T02
	SMR 1 AI	5.35/10.74	55.58	235.30	2022.204	T02
	HZE 4 AJ	2.25/12.43	23.12	276.28	2022.204	T02
	SMR 40 AO	5.35/12.65	180.06	274.21	2022.204	T02
	SMR 40 AP	5.35/12.84	169.58	282.13	2022.204	T02
	SMR 40 AQ	5.35/13.19	78.21	292.28	2022.204	T02
	STF 2758 BC	6.05/10.03	859.27	221.89	2022.204	T02
	FYM 106 BM	6.05/14.30	102.25	238.22	2022.204	T02
	FYM 106 BN	6.05/14.40	47.93	152.84	2022.204	T02
21070+3839	ES 2059	10.11/12.70	6.81	266.50	2022.209	T02
21071+3852	MLB 888	11.60/13.20	3.97	54.52	2022.209	T02
21071+3905	ALI 960	12.60/12.60	12.92	109.68	2022.209	T02
21072+3841	MLB 1018	12.30/13.70	4.40	252.02	2022.204	T02
21073+3857	MLB 889	10.20/11.50	7.01	5.17	2022.204	T02
21074+3841	MLB 1019	12.10/13.50	4.26	226.43	2022.204	T02
21074+3853	MLB 890	12.69/11.60	5.29	250.11	2022.204	T02
21075+3831	SEI 1408	11.10/11.80	9.27	53.58	2022.204	T02
21078+3834	BRT 2233	11.90/12.40	3.86	38.48	2022.209	T02

3.1. WDS 02094-1011: Components A and B are stars, components C, D, E, F are galaxy nuclei.

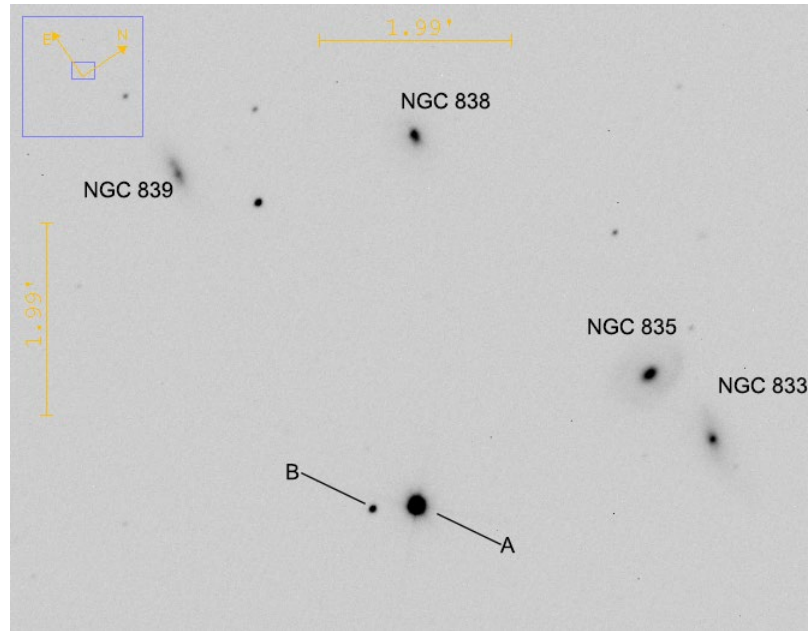


Figure 1: The WDS 02094-1011 and its environment in the image of the T33 telescope.

3.2. WDS 02470-0952: The members AB and CD are too close, they do not separate in the picture.

3.3. WDS 16542-4150: The system was last measured in 1999.

3.4. WDS 17190-3459: The AB components are too close and do not separate in the picture. Therefore, I could not measure BC and BC components. The last measurement of the AD and CD members was made in 1999.

3.5. WDS18176-3406: The last measurement of the AB and AC members was made in 1999.

3.6. WDS18242-3423: The AC components are too close. The last measurement of the AB and AD members was made in 1999.

3.7. WDS 18492+1813: The C component is much closed, I could not measure it.

3.8. WDS 19307+2758: The L component is lost in the pixels of the main star; I was unable to measure it.

3.9. WDS 19321+2816: Extremely close components, the probability of a measurement error is high.

New Double star at $18^{\text{h}} 00^{\text{m}} 53.13^{\text{s}} +56^{\circ}24^{\text{m}} 27.20^{\text{s}}$

The possible binary star is located $17'$ from the STF 2278 system in the constellation Dragon at 265° .

They can be found in the SIMBAD database under the identifier TYC 3911-235-1 and TYC 3911-106-1.

I obtained the following characteristics for the two stars with the Plot_Tool excel spreadsheet from the data of the GAIA EDR3 database.

Table 3: Star Condition

Star	Aver. mag	Abs Mag	Lum (\odot)	T eff K°	Rad (\odot)	Mass (\odot)
TYC 3911-235-1	11.80	3,32	4,04	6250	1,93	3.48
TYC 3911-106-1	11.86	3,39	3,77	5750	1,95	3.37

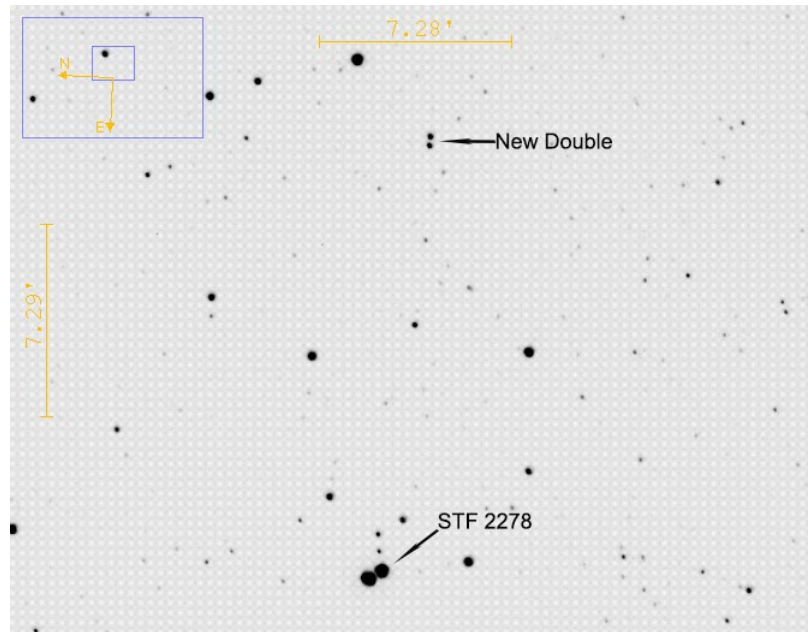


Figure 2: Image of the STF 2278 with new double star

For their distance from the Earth, taking into account the parallax error, in the case of member A, I got a minimum distance of 445 pc, a maximum distance of 501 pc, and a medium distance of 471 pc. In the case of member B these data are: 464; 523; 493 pc. It can be seen that the members are spatially very close to each other. The mean distance of the system from our Earth is 482 pc, and the mean distance of the members is 9,848 AU.

Table 4: My Measurement Data

Separation "	Position angle °	ΔM
50.44	87.39	0.24

4. Discussion

In general, it can be said that my current measurements agree with the latest data in the WDS catalog within the margin of error. In general, it can be said that my current measurements agree within the margin of error with the latest data in the WDS catalog. In the case of STF 308, HJ 4935, SEE 351, SMA 81, STFA 43, some members did not separate, I could not measure them. A greater difference was observed in the case of the pairs measured a long time ago.

Acknowledgements

This Research has made use of the Washington Double Star Catalog maintained at the U.S. Naval Observatory.

This Research has made use of the SIMBAD database, operated at CDS, Strasbourg, France
 This work has made use of data from the European Space Agency (ESA) mission Gaia (<https://www.cosmos.esa.int/gaia>), processed by the Gaia Data Processing and Analysis Consortium (DPAC, <https://www.cosmos.esa.int/web/gaia/dpac/consortium>). Funding for the DPAC has been

provided by national institutions, in particular the institutions participating in the Gaia Multilateral Agreement.

References

Harshaw, Richard, 2020, Using Plot Tool 3.19 to Generate Graphical Representations of the Historical Measurement Data, *JDSO*, **16**, No.4;386-400

Harfenist Steven A., 2018, Astrometric Measurements of Double Stars Using AstromImageJ and Astrometry.Net, *JDSO*, **14**, No.3;538-542

Mason, B.D., Wycoff, G.L. and Hartkopf, W.I. (2020), The Washington Double Star Catalog, Astrometry Department, U.S. Naval Observatory, <http://www.astro.gsu.edu/wds/>

SIMBAD <http://simbad.cds.unistra.fr/simbad/sim-fid>

Aladin lite <https://aladin.u-strasbg.fr/AladinLite/>

Stelle Doppie <https://www.stelledoppie.it/index2.php?section=1>

AstroimageJ <https://www.astro.louisville.edu/software/astroimagej/>